Journal of Materials Chemistry C

RSC Publishing

COMMUNICATION

View Article Online
View Journal | View Issue

Board-like dibenzo[*fg*,*op*]naphthacenes: synthesis, characterization, self-assembly, and liquid crystallinity†

Cite this: *J. Mater. Chem. C*, 2013, **1**, 5833

Received 13th July 2013
Accepted 9th August 2013

DOI: 10.1039/c3tc31353k

www.rsc.org/MaterialsC

Jian He,[a] Dena M. Agra-Kooijman,[b] Gautam Singh,[b] Chen Wang,[c] Cherrelle Dugger,[a] Jianbo Zeng,[a] Ling Zang,[c] Satyendra Kumar[b] and C. Scott Hartley*[a]

We report the synthesis and characterization of a series of board-like ("sanidic") compounds with dibenzo[*fg*,*op*]naphthacene cores. The compounds exhibit good self-assembly into one-dimensional belt-like structures, and also smectic liquid crystal phases typical of rod-like molecules, but with important differences ascribed to their board-like shapes.

Although the majority of small molecules exhibiting liquid crystal phases can be described as either rod-like (calamitic) or disc-like (discotic), many exceptions are known, underscoring the potential of other structural classes to exhibit new and unusual phase behavior. Board-like ("sanidic") compounds have long represented an interesting class of potential mesogens with proposed applications in high performance light modulators[1] and semiconducting thin films.[2] However, board-like small-molecule liquid crystals are quite uncommon, presumably, at least in part, because the synthesis of appropriately substituted cores is less straightforward than the synthesis of the cores typical of calamitics (*e.g.*, biaryls) and discotics (*e.g.*, triphenylenes). To date, the liquid crystal phases of reported[3–10] small-molecule compounds have typically been characterized by columnar stacking, by analogy with discotics.

ortho-Phenylene oligomers have recently been examined as simple polyphenylenes that fold into helices.[11,12] Their use as substrates for planarization[13] is an attractive goal, as the resulting board-like structures, shown in Fig. 1, would incorporate both biaryl and triphenylene subunits and should therefore be interesting candidates for liquid crystal behavior. Unfortunately, the direct oxidative planarization of even very short *o*-phenylenes is known to be problematic because of skeletal rearrangements.[14] To our knowledge, this synthetic challenge has yet to be overcome for the general case of *o*-phenylene oligomers. However, even short segments of the structure shown in Fig. 1 have the potential for self-assembly into interesting nanostructures and liquid crystal phases.

As a first step in investigating their properties, here we report the synthesis and characterization of the shortest possible planarized *o*-phenylenes of this type, **DBN(OR)**. Our synthesis is shown in Scheme 1. Although direct oxidative planarization of similar *o*-phenylene tetramers is known, albeit low-yielding,[15] it does not work at all for the synthesis of **DBN(OR)** because of rearrangements.[16] In our synthesis, this challenge is avoided through the use of chloro groups to direct a photochemical dehydrohalogenation, a reaction that had been previously reported for the synthesis of the parent compound.[17] Characterization of *o*-phenylene synthetic intermediates **1–3(OR)** is complicated by NMR spectral broadening because of slow conformational exchange, as expected (ESI†).[18] This broadening is, of course, lost on planarization to **DBN(OR)**. The NMR spectra are consistent with the symmetry and substitution pattern proposed for **DBN(OR)**, which was further confirmed by DFT predictions of the ^{13}C chemical shifts (ESI†). The compounds with *n*-alkoxy side-chains (**DBN(OC_6)**, **DBN(OC_8)**, **DBN(OC_{10})**, and **DBN(OC_{12})**) exhibit modest (but workable) solubility in common organic solvents, whereas **DBN(OC_{br})** exhibits very good solubility. There is no evidence in the NMR

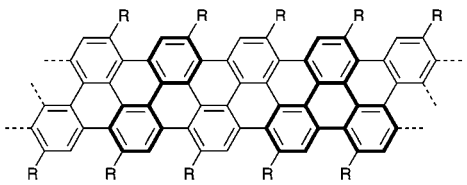

Fig. 1 Structure of a planarized *o*-phenylene. Biaryl (left) and triphenylene (right) subunits, typical of liquid crystals, are shown in bold.

[a]*Department of Chemistry & Biochemistry, Miami University, 651 E. High St., Oxford, Ohio 45056, USA. E-mail: scott.hartley@miamioh.edu*

[b]*Department of Physics, Kent State University, Kent, Ohio 44242, USA*

[c]*Department of Materials Science and Engineering, University of Utah, Salt Lake City, Utah 84108, USA*

† Electronic supplementary information (ESI) available: Supplemental figures, experimental procedures, and NMR spectra of new compounds. See DOI: 10.1039/c3tc31353k

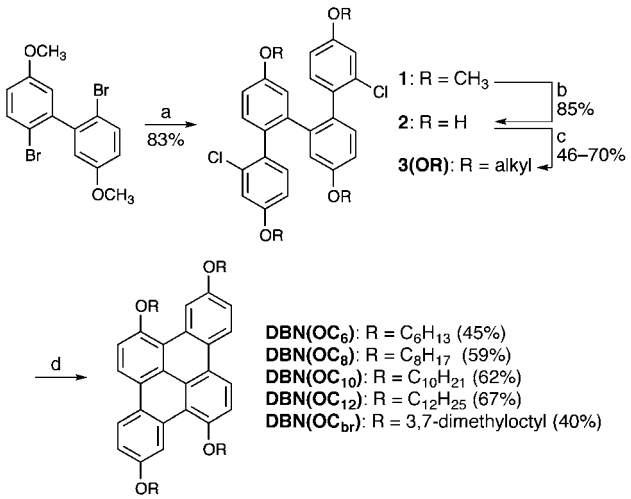

Scheme 1 *Reagents and conditions*: (a) 2-chloro-4-methoxyphenylboronic acid, $Pd(PPh_3)_4$, 2 M Na_2CO_3, toluene/EtOH, 90–100 °C; (b) BBr_3, CH_2Cl_2, −78 °C; (c) bromoalkane, K_2CO_3, DMF, 90 °C; (d) $h\nu$, benzene.

spectra for solution-phase aggregation of any of the compounds (*i.e.*, no concentration-dependent changes in chemical shifts).

We chose to focus on the more-soluble **DBN(OC$_{br}$)** for photophysical and electrochemical characterization, as the nature of the alkoxy groups should have little effect on the intrinsic properties of the dibenzo[*fg*,*op*]naphthacene (DBN) core (*e.g.*, the UV/vis and fluorescence spectra of **DBN(OC$_6$)**, shown in the ESI,† are identical to those of **DBN(OC$_{br}$)**). Its UV/vis and fluorescence spectra, shown in Fig. 2, are very similar to those of the parent (unsubstituted)[19] and other alkoxy-substituted[20] DBNs, and show minimal solvent dependence (ESI†). The compounds are highly fluorescent, with a quantum yield of $\Phi_f = 0.41$ for **DBN(OC$_{br}$)** in CH_2Cl_2 measured relative to 9,10-diphenylanthracene (excitation at 366 nm). Compound **DBN(OC$_{br}$)** in CH_2Cl_2 exhibits two oxidation waves in its cyclic voltammogram, shown in Fig. 3, at 0.35 and 0.88 V relative to the ferrocene/ferrocenium redox couple. These waves meet the criteria for electrochemical reversibility at a various scan rates between 50 and 500 mV s^{-1} (ESI†). Taking −4.8 eV as the HOMO level of ferrocene, the HOMO of **DBN(OC$_{br}$)** therefore lies at approximately −5.2 eV. The optical gap measured at the crossing point between the UV/vis and fluorescence spectra is 3.04 eV; thus, the LUMO lies at roughly −2.1 eV. Optimization of the geometry of a simplified methoxy-substituted derivative by DFT (B3LYP/6-31G(d)), shown in Fig. 4, indicates that the DBN core is not perfectly planar but rather is of C_2 symmetry, with a slight ruffling resulting from steric interactions between the alkoxy groups and the opposing hydrogens in the bay regions.

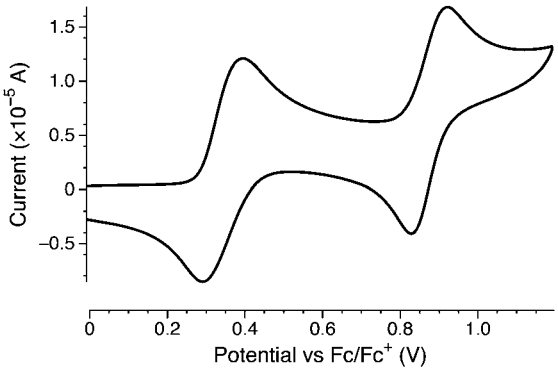

Fig. 3 Cyclic voltammogram of **DBN(OC$_{br}$)** in anhydrous CH_2Cl_2 with 0.1 M $^nBu_4NPF_6$ as supporting electrolyte at a scan rate of 100 mV s^{-1}.

The compounds with *n*-alkoxy side-chains show good self-assembly into one-dimensional nanostructures on crystallization from solution, as exemplified by the behavior of **DBN(OC$_{12}$)**. Slow cooling of a chloroform solution gives a gel consisting of fluorescent, belt-like fibers roughly 200 nm thick, 1 μm wide, and hundreds of μm long, shown in Fig. 5 and in the ESI.† To test their photoconductivity, the fibers of **DBN(OC$_{12}$)** were dispersed onto 20 μm gold electrodes separated by 5 μm. In the dark, the pristine fibers exhibited a current of 27 pA which increased 15-fold on irradiation with white light (65.9 mW cm^{-2}). The photocurrent was enhanced when electron-acceptor *N*,*N*′-dicyclohexylperylenediimide (PDI) was dropcast onto the substrate (0.15 mM, 100 μL in CH_2Cl_2), with a dark current of 371 pA which increased 65-fold to 24.2 nA on irradiation. PDI does not itself assemble into fiber-like structures under these conditions. A control experiment in which the PDI was dropcast onto the same electrode geometry in the absence of **DBN(OC$_{12}$)** showed a photocurrent of only 15 pA, representing a ∼4-fold enhancement (ESI†). As **DBN(OC$_{12}$)** exhibits only low solubility in CH_2Cl_2, the enhancement

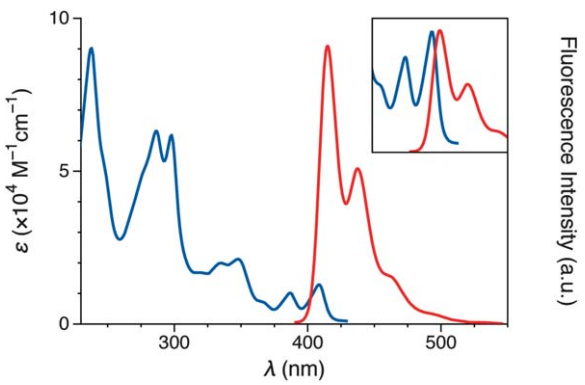

Fig. 2 UV/vis (blue, left) and fluorescence (red, right) spectra of **DBN(OC$_{br}$)** in dilute CH_2Cl_2. Inset: direct comparison of the fluorescence spectrum and the red-edge of the UV/vis spectrum.

Fig. 4 Optimized geometry (B3LYP/6-31G(d)) of the methoxy-substituted dibenzo[*fg*,*op*]naphthacene core.

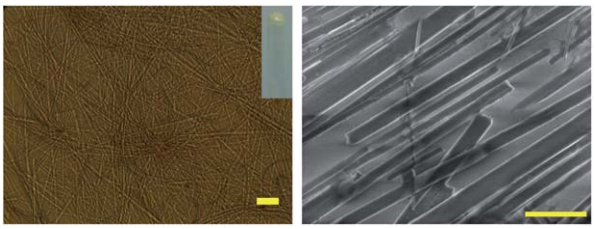

Fig. 5 Left: bright field image of **DBN(OC$_{12}$)** fibers (scale bar: 20 μm); inset: gelation product. Right: SEM image of the fibers (scale bar: 4 μm).

presumably arises from coating of the fibers with PDI layers,[21] leading to efficient charge separation though enhanced absorption of white light by the PDI followed by a favorable HOMO–HOMO charge transfer.

The thermal behavior of the compounds was investigated by differential scanning calorimetry (DSC), polarized optical microscopy (POM), and X-ray diffraction (XRD). Phase transitions of the four compounds with *n*-alkoxy side-chains are given in Table 1; the DSC, POM, and XRD data are shown in the ESI.† On cooling from the isotropic liquid, compounds **DBN(OC$_6$)** and **DBN(OC$_8$)** both exhibit the smectic A (SmA) liquid crystal phase, a fluid in which the constituent molecules are, on the time-average, arranged in layers with their long axes parallel to the layer normal. The SmA phase was identified by a mixture of focal conic textures and optically isotropic homeotropic regions observed by POM. XRD patterns of the materials in the liquid crystalline states are typical of the SmA phase, with sharp peaks at small angle corresponding to layer spacings of 24.7 and 27.6 Å, respectively, against estimated molecular lengths of 26 and 30 Å in fully extended conformations; the only other feature in both cases is the usual diffuse maximum at ~4.5 Å corresponding to the packing of molten alkyl chains. Compound **DBN(OC$_{12}$)** also exhibits a single liquid crystal phase that was identified as the tilted smectic C (SmC) phase, which is structurally similar to the SmA except that the molecules are tilted from the layer normal. The SmC phase was identified by characteristic broken focal conic and schlieren textures by POM. The XRD pattern indicates a layer spacing of 31.6 Å (the estimated molecular length is 40 Å), along with corresponding higher-order peaks. The falling of clearing point temperatures and shift from the SmA to the SmC phase with increasing side-chain length is typical of calamitic mesogens.[22]

Table 1 Phase behavior of **DBN(OC$_6$)**, **DBN(OC$_8$)**, **DBN(OC$_{10}$)**, and **DBN(OC$_{12}$)**

Compound	Transition temperatures[a] (°C) [enthalpies (kJ mol^{-1})]							
DBN(OC$_6$)	Heat: Cr	220 [21]	SmA	222 [8]	I			
	Cool: Cr	208 [20]	SmA	222 [9]	I			
DBN(OC$_8$)	Heat: Cr			201 [32]	I			
	Cool: Cr	197 [24]	SmA	201 [7]	I			
DBN(OC$_{10}$)	Heat: Cr	180 [25]			SmA	184 [5]	I	
	Cool: Cr	176 [19]	SmC	180 [4]	SmA	183 [5]	I	
DBN(OC$_{12}$)	Heat: Cr	162 [19]	SmC	165 [9]	I			
	Cool: Cr	160 [19]	SmC	165 [9]	I			

[a] 5 K min^{-1}.

Compound **DBN(OC$_{10}$)** exhibits both the SmA and SmC phases, and thus was considered more carefully in order to contrast their properties in this series of compounds. Unusually,[23] the SmA–SmC transition appears to be first-order, with a clear peak in the DSC trace corresponding to a transition enthalpy of 4.2 kJ mol^{-1}. Further support of the first-order nature of the SmA–SmC transition is given by the non-zero transition enthalpy when extrapolated to a scan rate of 0.[24] The molecular tilt in the SmC phase, as determined by XRD, is ~12° and essentially constant over the (narrow) phase range. The layer spacing in the SmA phase is approximately 29.2 Å, decreasing to 28–29 Å in the SmC phase (molecular length 35 Å). Polarized microscopy images of the two phases are compared in Fig. 6 for the same region of the film. The appearance of the SmC phase is indicated by the conversion of the focal conic to broken focal conic textures (along with a pronounced increase in birefringence) and the appearance of schlieren textures from the homeotropic domains.

Other reported mesogens based on the same DBN core exhibit columnar (discotic) liquid crystal phases.[15,25,26] These other examples have more side-chains (6 or 8), which are arranged symmetrically around the core; in the **DBN(OR)** series, the compounds have only 4 *n*-alkoxy side-chains with no interface curvature[27] between the aryl and alkoxy blocks, which should favor lamellar packing (*i.e.*, they are more board-like). The phase behavior of these new compounds contrasts with that of other reported board-like small-molecule mesogens. Notably, unlike most[3–8] of these other cases (with the notable exception of certain metallomesogens[9,10]), there is no evidence of columnar stacking in the phases exhibited by the **DBN(OR)** series. This is an important distinction as the technological potential of board-like mesogens is often presented in terms of non-columnar phases. That said, although the phases observed here are similar to those expected for common calamitics, our (preliminary) characterization does suggest some important differences attributable to the board-like shape of the **DBN(OR)** compounds. The first-order SmA–SmC phase transition associated with a large increase in birefringence suggests a significant increase in core ordering when the molecules tilt; in other words, in contrast to the typical SmC phase of tilted rods, the cores of the constituent molecules here may become ordered along their short axes. Such a "doubly biaxial"[7,28] SmC phase could be of interest in organic semiconducting films if better core–core correlations translates to better (semi)conductivity. Further investigations into the precise structure of these phases are ongoing.

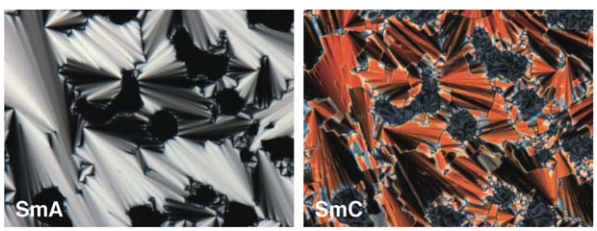

Fig. 6 Polarized microscopy images of a thin film of **DBN(OC$_{10}$)**. The same region of the sample is imaged in both cases.

C.S.H., J.H., and C.D. acknowledge support from the National Science Foundation (CHE-0910477 and CHE-1004875) and the Air Force Office of Scientific Research (FA9550-10-1-0377). Structural X-ray investigations were performed by D.M.A.-K., G.S., and S.K. with support from the Office of Basic Energy Sciences, Office of Science, U.S. Department of Energy under grant DE-SC00001412 at the National Synchrotron Light Source, Brookhaven National Laboratory supported under Contract no. DE-AC02-98CH10886. C.W. and L.Z. acknowledge the support of DHS (2009-ST-108-LR0005) and NSF (CHE 0931466).

Notes and references

1 R. Berardi, L. Muccioli and C. Zannoni, *J. Chem. Phys.*, 2008, **128**, 024905.
2 W. Pisula, M. Zorn, J. Y. Chang, K. Müllen and R. Zentel, *Macromol. Rapid Commun.*, 2009, **30**, 1179–1202.
3 D.-Y. Kim, L. Wang, Y. Cao, X. Yu, S. Z. D. Cheng, S.-W. Kuo, D.-H. Song, S. H. Lee, M.-H. Lee and K.-U. Jeong, *J. Mater. Chem.*, 2012, **22**, 16382–16389.
4 M. Artal, K. Toyne, J. Goodby, J. Barbera and D. Photinos, *J. Mater. Chem.*, 2001, **11**, 2801–2807.
5 R. Chaudhuri, M.-Y. Hsu, C.-W. Li, C.-I. Wang, C.-J. Chen, C. K. Lai, L.-Y. Chen, S.-H. Liu, C.-C. Wu and R.-S. Liu, *Org. Lett.*, 2008, **10**, 3053–3056.
6 D. Haristoy, S. Mery, B. Heinrich, L. Mager, J. F. Nicoud and D. Guillon, *Liq. Cryst.*, 2000, **27**, 321–328.
7 A. Mori, M. Yokoo, M. Hashimoto, S. Ujiie, S. Diele, U. Baumeister and C. Tschierske, *J. Am. Chem. Soc.*, 2003, **125**, 6620–6621.
8 C. W. Struijk, A. B. Sieval, J. E. J. Dakhorst, M. van Dijk, P. Kimkes, R. B. M. Koehorst, H. Donker, T. J. Schaafsma, S. J. Picken, A. M. van de Craats, J. M. Warman, H. Zuilhof and E. J. R. Sudhölter, *J. Am. Chem. Soc.*, 2000, **122**, 11057–11066.
9 M. Ghedini, I. Aiello, A. Crispini, A. Golemme, M. La Deda and D. Pucci, *Coord. Chem. Rev.*, 2006, **250**, 1373–1390.
10 M. J. Baena, P. Espinet, M. B. Ros, J. L. Serrano and A. Ezcurra, *Angew. Chem., Int. Ed. Engl.*, 1993, **32**, 1203–1205.
11 S. M. Mathew, J. T. Engle, C. J. Ziegler and C. S. Hartley, *J. Am. Chem. Soc.*, 2013, **135**, 6714–6722.
12 S. Ando, E. Ohta, A. Kosaka, D. Hashizume, H. Koshino, T. Fukushima and T. Aida, *J. Am. Chem. Soc.*, 2012, **134**, 11084–11087.
13 J. Wu, W. Pisula and K. Müllen, *Chem. Rev.*, 2007, **107**, 718–747.
14 J. L. Ormsby, T. D. Black, C. L. Hilton, Bharat and B. T. King, *Tetrahedron*, 2008, **64**, 11370–11378.
15 S. Kumar, J. Naidu and D. Rao, *J. Mater. Chem.*, 2002, **12**, 1335–1341.
16 J. L. Crase, MS thesis, Miami University, 2010.
17 T. Sato, S. Shimada and K. Hata, *Bull. Chem. Soc. Jpn.*, 1971, **44**, 2484–2490.
18 C. S. Hartley and J. He, *J. Org. Chem.*, 2010, **75**, 8627–8636.
19 R. Schoental and E. J. Y. Scott, *J. Chem. Soc.*, 1949, 1683–1696.
20 P. Uznanski, S. Marguet, D. Markovitsi, P. Schuhmacher and H. Ringsdorf, *Mol. Cryst. Liq. Cryst.*, 1997, **293**, 123–133.
21 Y. Che, H. Huang, M. Xu, C. Zhang, B. R. Bunes, X. Yang and L. Zang, *J. Am. Chem. Soc.*, 2011, **133**, 1087–1091.
22 M. E. Neubert, in *Liquid Crystals: Experimental Study of Physical Properties and Phase Transitions*, ed. S. Kumar, Cambridge University Press, Cambridge, 2001, pp. 393–476.
23 C. C. Huang, in *Handbook of Liquid Crystals*, ed. D. Demus, J. Goodby, G. W. Gray, H. Spiess and V. Vill, Wiley-VCH, Weinheim, 1998, vol. 2A, pp. 441–469.
24 V. N. Raja, R. Shashidhar, B. R. Ratna, G. Heppke and C. Bahr, *Phys. Rev. A*, 1988, **37**, 303–305.
25 P. Henderson, H. Ringsdorf and P. Schuhmacher, *Liq. Cryst.*, 1995, **18**, 191–195.
26 H. Bock and W. Helfrich, *Liq. Cryst.*, 1992, **12**, 697–703.
27 C. Tschierske, *J. Mater. Chem.*, 1998, **8**, 1485–1508.
28 C. Tschierske and D. J. Photinos, *J. Mater. Chem.*, 2010, **20**, 4263–4294.

